UNIVERSITY OF CALIFORNIA, SAN DIEGO

Osteopontin knockout abates high fat diet-induced insulin resistance and adipose tissue inflammation

A Thesis submitted in partial satisfaction of the requirements for the degree Master of Science

in

Biology

by

Divya Thapar

Committee in charge:

Professor Dorothy D. Sears, Chair
Professor Stephen M. Hedrick, Co-chair
Professor Colin C. Jamora

2008

The Thesis of Divya Thapar is approved and it is acceptable in quality and form for publication on microfilm and electronically:

_____

_____

_____

Chair

University of California, San Diego

2008

DEDICATION

To all the friends, family and co-workers that continued to encourage me throughout this long process. I especially thank my parents and brother who supported me in this endeavor. Without all of you I do not think this day would ever have come. And to all of you for reminding me that I would, eventually, graduate.

EPIGRAPH

The advantage of a bad memory is that one enjoys several times the same good things for the first time.

Friedrich Nietsche

The most exciting phrase to hear in science, the one that heralds the most discoveries, is not Eureka! (I found it!) but 'That's funny…'

Isaac Asimov

Life is far too important a thing ever to talk seriously about.

Oscar Wilde

TABLE OF CONTENTS

LIST OF ABBREVIATIONS

ATM	Adipose tissue macrophage
ECM	Extracellular matrix
eWAT	Epididymal white adipose tissue
FACS	Fluorescent-activated cell sorting
FFA	Free fatty acid
GDR	Glucose disposal rate
GIR	Glucose infusion rate
HFD	High fat diet
HGO	Hepatic glucose output
IFNγ	Interferon γ
IKKβ	IκB kinase β
IL	Interleukin
IR	Insulin receptor
IRS	Insulin receptor substrate
iWAT	Inguinal white adipose tissue
JNK	c-Jun N-terminal kinase

KO	Knockout
MCP-1	Monocyte chemotactic protein-1
MMP	Matrix-metalloproteinase
NC	Normal chow
OGGT	Oral glucose tolerance test
OPN	Osteopontin
PDK-1	Phosphatidylinositol-3,4,5-triphosphate-dependent kinase 1
PI 3-K	Phosphoinositide 3-kinase
PTM	Post-translational modification
qPCR	Quantitative polymerase chain reaction
RGD	Arginine-glycine-aspartate
SPP1	Secreted phosphoprotein 1
SVF	Stromal vascular fraction
T2D	Type 2 Diabetes
TNFα	Tumor necrosis factor α
WAT	White adipose tissue
WT	Wild type

LIST OF FIGURES

ACKNOWLEDGEMENTS

I first and foremost would like to acknowledge Dorothy D. Sears and Justin Chapman for helping me throughout this two-year long process. You both stuck by me and encouraged me through all the difficulties of stupid pin-worm mice and those 3T3s that just did not work. Both of you were there from the beginning when I did not even know what osteopontin was and guided me through the process to having the understanding that I do now. I will forever be grateful.

Secondly, I would like to acknowledge my committee members, Drs. Hedrick and Jamora. Because I know serving on a master's committee is not the most desirable post to take upon.

I would also like to acknowledge Jachelle O. Pimentel, Saswata Talukdar, and Anh-Khoi Nguyen for teaching me how survive in the lab. From showing me how to "pour" an SDS-PAGE gel, find things in the lab, and figure out what to do with the mice. Without your help, none of this would be possible.

I must acknowledge the members of the Olefsky Lab as well as Trisha Haubrich of the Chapman Lab for overall guidance and support in this long journey.

I thank the following for their assistance: Dennis J. Young for assistance with FACS analysis, Laarni Gapuz for histological analysis, and Margo Streets for metabolic chamber analysis.

I thank Chris Hupfeld for use of his GAPDH and IL-6 primers. I also thank Min Lu for use of his RNA Polymerase II primers.

Results, Section 1, in part is currently being prepared for submission for publication of the material. Divya Thapar, the thesis author, is a co-author of this material. I acknowledge Dorothy D. Sears, Justin G. Chapman, Jachelle M. Ofrecio, Philip D. Miles and Jaap G. Neels as co-authors of this material.

Results, Section 2, in part is currently being prepared for submission for publication of the material. Divya Thapar, the thesis author, is a co-author of this material. I acknowledge Dorothy D. Sears, Saswata Talukdar, and Jachelle M. Ofrecio as co-authors of this material.

ABSTRACT OF THE THESIS

Osteopontin knockout abates high fat diet-induced insulin resistance and adipose tissue inflammation

by

Divya Thapar

Master of Science in Biology

University of California, San Diego, 2008

Professor Dorothy D. Sears, Chair

In recent years type 2 diabetes has been shown to consist of not only insulin resistance of insulin target tissues (muscle, adipose tissue, and liver) but inflammation of adipose tissue as well. This inflammatory state is characterized by increased macrophage infiltration and pro-inflammatory cytokine expression. Given the known pro-inflammatory roles of osteopontin in many pathological states in addition to its cell

migration enhancing properties, osteopontin was examined for its effect on diet-induced obesity. Osteopontin knockout mice exhibited increased liver insulin sensitivity by hyperinsulinemic euglycemic clamp after two and 16 weeks on high fat diet compared to the wild type mice. Increased muscle insulin sensitivity was also observable after two weeks on diet by clamp in the knockout mice. Enhanced insulin signaling in muscle, adipose tissue, and liver, assessed by Akt phosphorylation, was also observed in the osteopontin knockout mice versus the wild type mice after high fat feeding, indicating attenuated insulin resistance. Osteopontin knockout mice also showed diminished adipose tissue hypertrophy, triple-positive pro-inflammatory cell infiltration into adipose tissue, and inflammatory cytokine expression, indicating less inflammation of the adipose tissue after short-term high fat diet. Total osteopontin expression as well as differential isomeric expression of it in the adipose tissue was observed to increase after high-fat diet in wild type mice, further implicating its role in inflammation of the adipose tissue. Osteopontin appears to mediate the effects of short- and long-term diet-induced obesity in a cytokine-like manner, leading to localized inflammation of the adipose tissue which results in systemic insulin resistance.

INTRODUCTION

Type 2 diabetes and insulin resistance

Type 2 diabetes (T2D) consists primarily of two components: insulin resistance and diminished β-cell function (11). Its incidence in both the youth and adult populations has increased dramatically in the last twenty years, largely due to the increased prevalence of obesity (32). Insulin resistance is a state in which greater than normal amounts of insulin are required to regulate glucose homeostasis in insulin target tissues, including liver, skeletal muscle, and adipose tissue (30); it is believed to be the precursory defect that leads to loss of β-cell function and eventual full blown T2D (25). It is thought that insulin resistance occurs in the prediabetic state, leading to hyperinsulinemia as compensation by the β-cells' secretion machinery. At this point glucose tolerance functions properly. Eventually, the prolonged state of hyperinsulinemia causes a deterioration of the β-cells' response and insulin insufficiency develops. Insulin insufficiency in conjunction with the insulin resistance leads to a state of glucose intolerance and hyperglycemia and what is defined as full-blown T2D (25).

Insulin resistance is the primary defect leading to T2D and is one of several pathologies with a high rate of comorbidity termed "syndrome X" or the "metabolic syndrome." Although there is no strict definition of syndrome X, it includes the following pathologies: insulin resistance, hyperinsulinemia, dyslipidemia (usually high triglyceride levels and low HDL levels), hypertension, hyperuricemia, and increased cardiovascular disease propensity among other things (26, 25). Insulin resistance is also associated with non-T2D diseases such as polycystic ovarian syndrome, aging, and

simple obesity (25). Thus, understanding the mechanisms of insulin resistance in both T2D and other diseases is of great importance.

Diabetes - a global issue

Diabetes is a major public health issue of the 21st century. In 2007, it was estimated that 23.6 million people in the United States, 7.8% of the population, had some form of diabetes, including 5.7 million undiagnosed people (7). It is predicted that by the year 2030, 30.3 million people in the U.S. alone will have diagnosed diabetes (35). But this diabetes epidemic is not solely a national issue. The incidence of diabetes is rising on a global scale. As of 2000, India and China had 31.7 and 20.8 million people with diabetes, respectively; and are the countries with the largest population of people with diabetes. By 2030, India's diabetic population is expected to rise to 79.4 and China's to 42.3 million people, representing a 151% and 104% increase in the number of people with diabetes, respectively (35). Preventing diabetes is not only important for its impact on society in terms of health, but for its economic impact on society as well. In 2007 alone, it was estimated that $174 billion was spent in the United States on diabetes, including $58 billion in indirect costs (disability, work loss, premature mortality) (7). Research into and increased understanding of the causes of diabetes as well as the care and prevention of diabetes are imperatives for today's community.

Insulin signal transduction pathway

The actions of insulin control glucose and lipid metabolism through a defined signal transduction pathway that leads to glucose uptake and other metabolic alterations

in target cells. The relative amounts of signaling components and/or their degree of activation within the pathway can be used to indicate the ability of insulin to signal in response to different experimental conditions. The insulin signaling process begins with insulin receptor (IR), a trans-membrane protein with two functionally distinct domains. The binding of insulin to the extracellular domain causes the activation of the intracellular kinase. The IR has inherent tyrosine kinase activity that, when stimulated by insulin, causes tyrosine autophosphorylation of the receptor and phosphorylation on tyrosine residues of intracellular substrates including a family of proteins referred to as insulin receptor substrate-proteins (IRS-proteins). IRS-1 has been shown to be responsible for glucose uptake in muscle and adipose tissue, while IRS-2 has been shown to be active in the liver and β-cells (18). The phosphorylated tyrosine residues on IRS-1/2 bind multiple proteins with SH2 domains. The binding of IRS-1/2 to phosphoinositide 3-kinase (PI 3-kinase) at its regulatory subunit is the stimulus that leads to uptake of glucose and glycogen synthesis. Inhibition of PI 3-kinase inhibits insulin-induced glucose uptake as well as glycogen synthesis (4, references within). Activated PI 3-kinase leads to formation of phosphatidylinositol-3,4,5-triphosphate. Phosphatidylinositol-3,4,5-triphosphate in turn activates phosphatidylinositol-3,4,5-triphosphate-dependent kinase 1 (PDK1). PDK1 phosphorylates Akt at Thr308. It is presumed that another PDK phosphorylates Akt at Ser473. The double phosphorylation event results inhibition of glycogen synthase kinase-3 and activation of glycogen synthase and protein synthesis. Further mediating glucose homeostasis, Akt phosphorylation causes the translocation of the glucose transporter GLUT4 to the plasma membrane where glucose uptake occurs (3).

Given this signaling pathway, the amount of phosphorylated proteins after an insulin stimulus can be used as an indication of the ability of insulin to signal within the cell. Common proteins examined include phospho-Akt, phospho-IRS-1/2, and phospho-IR. It has previously been shown that the phosphorylation of IRS proteins by IR is defective in animals and humans with systemic insulin resistance. In addition, serine phosphorylation of IRS proteins by pro-inflammatory cytokines as well as other mediators of insulin resistance has been found to cause inhibition of IRS-1 in insulin signaling (13).

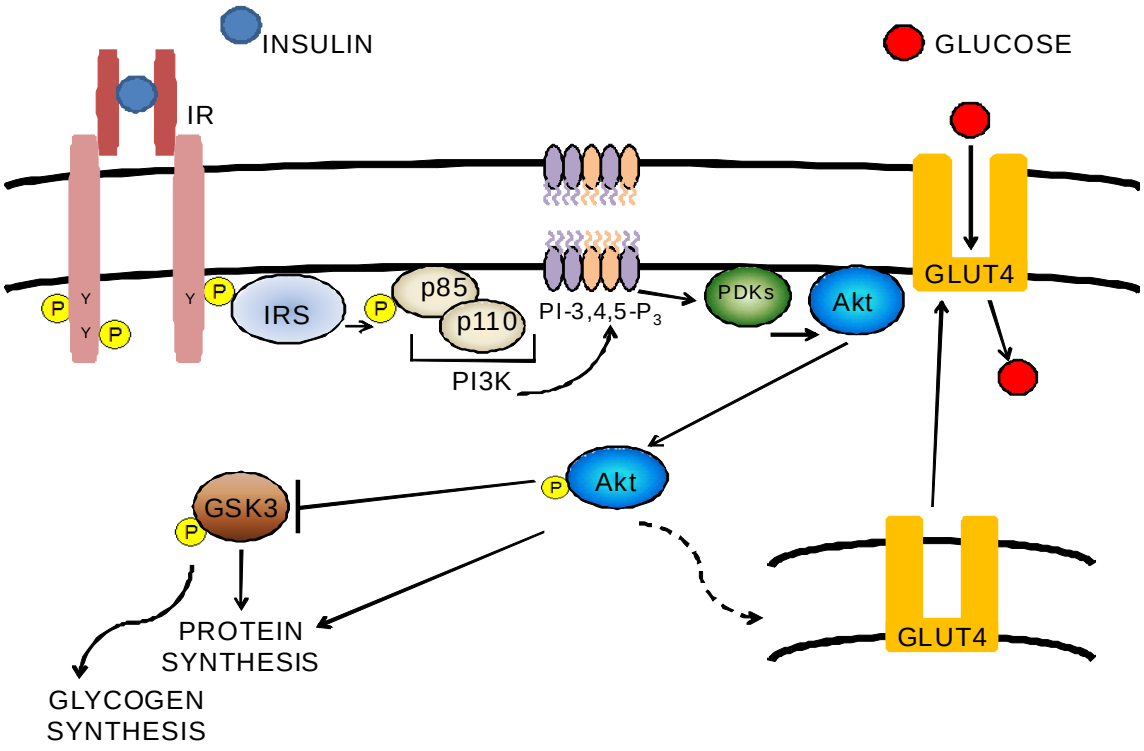

Figure 1. The insulin signal transduction pathway leading to GLUT4 translocation. Insulin binding to IR is shown activating a protein response cascade. The signal eventually leads to glycogen and protein synthesis and GLUT4 translocation to the cell membrane where glucose uptake into the cell occurs.

Insulin resistance and inflammation

As the incidence of T2D has risen concomitantly with obesity, more research has been devoted towards elucidating the relationship between obesity and insulin resistance. During the last several years, it has been found that both obesity and insulin resistance are associated with a state of chronic, low grade inflammation. Evidence shows that inflammation contributes in the development and progression of insulin resistance (32, 13). Adipose tissue, especially white adipose tissue (WAT), is a site of energy storage and liberation that consists of a heterogeneous population of cell types including adipocytes, preadipocytes, macrophages, and endothelial cells. Adipose tissue macrophages (ATMs) have been shown to increase with obesity and have a role in clearing adipocytes that have died from the hypoxic environment or high lipid load. This is more prevalent in the visceral depots of WAT as opposed to subcutaneous depots (28).

Free fatty acid (FFA) secretion increases during diet-induced obesity due to defective regulation of lipolysis. FFAs activate the c-Jun N-terminal kinase (JNK) and IκB kinase β (IKKβ) inflammatory pathways, thereby increasing the overall inflammatory state of the tissue and promoting insulin resistance (21, 39). High extracellular levels of FFAs in WAT act in a cytokine-like manner to induce inflammatory signaling within ATMs causing an attenuation of insulin sensitivity (22). Another result of inflammation that contributes to insulin resistance is adipocyte and macrophage cytokine secretion. Adipocytes secrete a number of adipokines that affect insulin sensitivity locally and systemically. Likewise, ATMs secrete cytokines that act in both an autocrine and paracrine manner to alter insulin sensitivity in adipose tissue (32).

One of the first discoveries to support this theory was the finding that tumor necrosis factor α (TNFα), a pro-inflammatory cytokine expressed by both macrophages and adipocytes, is overexpressed in the adipose tissue of obese mice and negatively affects insulin action (14; 30). The expression of inflammatory interleukins (ILs) is also increased in insulin resistance. The most notable of the inflammatory ILs is IL-1β and IL-6. IL-1β has been shown to lower expression of IRS-1 on both a transcriptional and post-transcriptional level (17). In doing so, IL-1β inhibits insulin signaling and further propagates insulin resistance. IL-6 expression has been shown to increase with insulin resistance and obesity; upon weight loss and improved insulin signaling, IL-6 expression decreases (19, 32). Together, these factors further indicate a role of inflammation in insulin resistance.

Expression of proteins involved in macrophage recruitment to the adipose tissue has also been shown to correlate with insulin resistance and obesity, supporting the role of inflammation and immune cell function in insulin sensitivity. The expression of monocyte chemotactic protein-1 (MCP-1), an adipocyte secreted chemoattractant, is elevated in the WAT of obese mice. Knockout (KO) of MCP-1 in mice has been shown to reduce macrophage infiltration into the adipose tissue as well as diminish diet-induced insulin resistance in the KO mice (34). Other proteins involved in macrophage migration that have been implicated in macrophage infiltration of adipose tissue are migration inhibitory factor (MIF) and macrophage inflammatory protein-1 (MIP-1) (32, 30).

The role of triple-positive pro-inflammatory immune cells in insulin resistance

Much research has been done to characterize the pro-inflammatory macrophages that infiltrate WAT and contribute to insulin resistance. Historically, F4/80 and CD11b are known to be cell-surface markers that identify macrophages, although, these markers have been shown to be expressed in several other immune cell types including natural killer cells and dendritic cells (20). Recent evidence shows that the macrophages that infiltrate the WAT and are activated in response to inflammatory stimulants express both the F4/80 and CD11b markers. In addition, these pro-inflammatory "macrophages" have been shown to express CD11c, a typical dendritic cell marker (22). These "triple-positive pro-inflammatory cells" display increased pro-inflammatory cytokine expression as well as macrophage chemotactic protein expression in response to FFAs. In contrast, the double-positive F4/80+, CD11b+, CD11c- cells show a much smaller response to FFA treatment. Expression of IL-1β, IL-6 and TNFα increases in F4/80+, CD11b+, CD11c+ cells and not in F4/80+, CD11b+, CD11c- cells after treatment with FFAs. The triple-positive pro-inflammatory cells are also increasingly present within the WAT (22). It is yet unclear what this triple-positive phenotype represents in terms of immune cell category. Possibilities include infiltration of novel immune cells displaying both macrophagic and dendritic traits into the WAT or conversion of adipose tissue resident F4/80+, CD11b+, CD11c- ATMs to F4/80+, CD11b+, CD11c+ cells. This data suggests that triple-positive pro-inflammatory cells are more directly involved in insulin resistance and inflammation in the WAT than generic macrophages.

Osteopontin

Osteopontin (OPN) is a secreted protein found ubiquitously in body fluids. The gene name for OPN is secreted phosphoprotein 1 (SPP1), but will only be referred to as OPN in this study. Its expression has been found to correlate with a number of pathologies including tumorigenesis, atherosclerotic plaque formation, and Crohn's disease (9, 6, 1). It is associated with the extracellular matrix (ECM) where it has roles in remodeling, cell adhesion, and cell migration (29). OPN binds to collagen and signals through multiple receptors (9). OPN binds to CD44 as well as various integrin receptors through an arginine-glycine-aspartate (RGD)-binding motif and other known integrin motifs present within its protein structure (Figure 2A) (16, 33).

OPN is a 32 kDa protein. Human OPN is known to have a number of splice variants. It undergoes extensive post-translation modification (PTM) due to multiple serine and threonine phosphorylation sites as well as N- and O-glycosylation sites within its sequence (Figure 2B) (9). It is further able to undergo PTM due to a thrombin cleavage site and various cleavage sites for matrix metalloproteinases (MMPs) including one within an integrin-binding motif (29). OPN is susceptible to cleavage by MMP-2, MMP-3, MMP-7, MMP-9, and MMP-12 (2, 15). Therefore, OPN function seems to be dependent on the extent and type of PTM.

OPN has a role in inflammation. It is highly expressed in macrophages and is known to act as a macrophage and T-cell chemotactic agent most notably in areas of inflammation (29, 38). Moreover, OPN has been shown to control macrophage adhesion, differentiation, phagocytosis and cytokine expression (29, and references within).

Previous studies by colleagues examined OPN expression in insulin resistant humans and rats. They found an elevation of OPN expression as insulin resistance within the subjects increased. After treatment with thiazoledinediones, insulin sensitizing drugs, OPN expression decreased (data unpublished). This further implicated OPN in having some role in insulin resistance, and led us to our current study. Together, the data implicates OPN as a good candidate for investigation into its role in insulin resistance

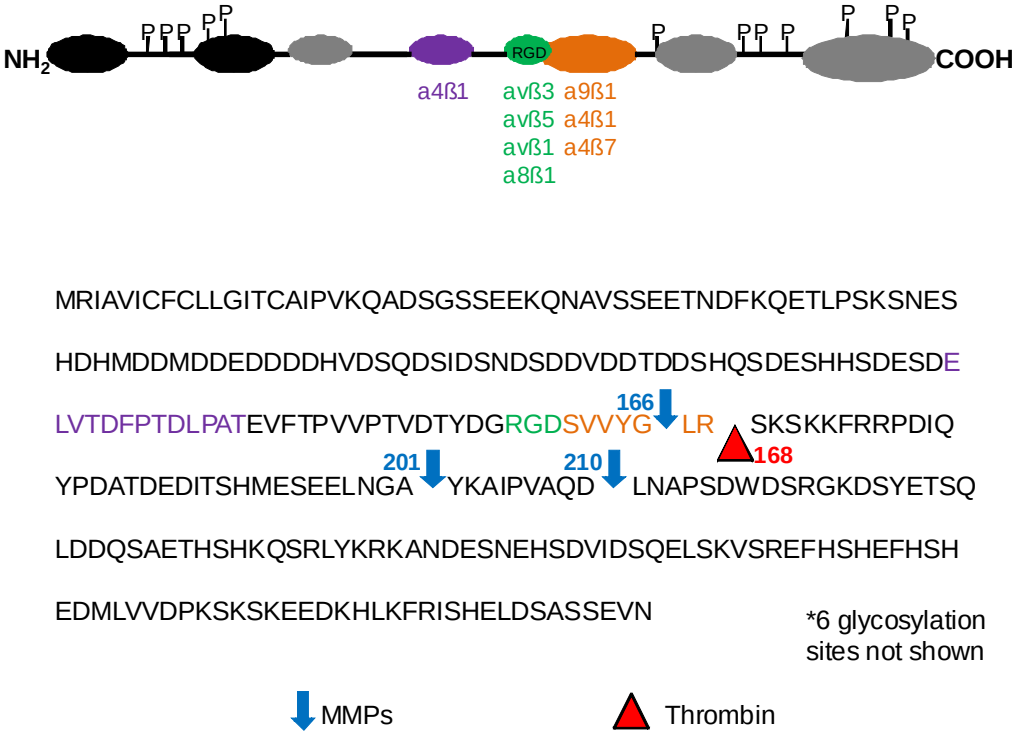

Figure 2. Schematic of CD44 and integrin receptor binding sites within OPN protein as well as phosphorylation sites. Human OPN protein sequence. Green RGD and purple and orange amino acid sequences indicate various integrin binding motifs. Blue arrows indicate cleavage sites of a number of MMPs. Red triangle indicates thrombin cleavage site. Serine and Threonine phosphorylation sites depicted.

Purpose of this study

This study examined the effects of an OPN knockout (KO) on insulin resistance and inflammation in a 2-16 week high fat diet (HFD) mouse model. OPN KO mice showed protection from insulin resistance in liver and muscle by hyperinsulinemic euglycemic clamp. Akt phosphorylation was also less inhibited in the OPN KO mice after acute insulin treatment. Inflammation of the adipose tissue was decreased in OPN KO mice. This was assessed by diminished cytokine expression, macrophage infiltration, and adipocyte hypertrophy in the WAT. We found that OPN is required for the development of insulin resistance and adipose tissue inflammation.

MATERIALS AND METHODS

Mice and Diet

C57Bl/6J WT mice (cat#000664) and OPN KO mice (B6.Cg-Spp1^{tm2blh}/J, cat # 004936) were purchased from Jackson Laboratories. The OPN KO mice are from a line that has been backcrossed into the C57Bl/6J background greater than 10 generations. Only male mice aged 3-7 months were utilized in this investigation and all mice were age-matched. All high fat diets (HFDs) were started at 12 or 16 weeks of age. Prior to this age all animals were fed normal chow diet (NC). The diets are as follows: NC is 12% kcal from fat (Purina 5001, LabDiet), 41% HFD is 41% kcal from fat (TD96132, Harlan Teklad), 60% HFD is 60% kcal from fat (D12492, Research Diets, Inc.). All mice were housed 1-4 per cage and under a controlled 12 light: 12 dark cycle as well as a controlled climate setting. The mice had access to food and water ad libitum. Procedures were approved by the University of California. All procedures were performed in accordance with the *Guide for Care and Use of Laboratory Animals* of the National Institutes of Health and were approved by the University of California, San Diego, Animal Subjects Committee.

Metabolic studies in mice – two week 41% HFD study

Insulin sensitivity in the mice was determined using a hyperinsulinemic euglycemic glucose clamp technique as previously described (12) with the following modifications: 1) isoflurane was used for anesthesia, 2) glucose tracer was infused at 2 μ Ci/hr, and 3) insulin was infused at 3 mU/kg/min. The animals were allowed to recover.

Four days later, mice were fasted for 5 hr and then anesthetized (isoflurane) to collect blood (cardiac puncture), and then euthanized (pentobarbital) to collect gastrocnemius muscle, liver, epididymal WAT (eWAT), and inguinal WAT (iWAT). Half of each tissue sample was flash-frozen in liquid nitrogen and half was fixed in Zn-formalin. Plasma glucose specific activity, GDR, GIR, and HGO were calculated as described above. Acute insulin stimulation was achieved by intraperitoneal injection of 6 hr-fasted mice with 0.85 U/kg insulin. After 15 min., tissues were harvested as above.

Metabolic studies in mice – two and four week 60% HFD study

Mice were anesthetized via intramuscular injection of a cocktail of ketamine HCl (100 mg/ml), xylazine (20 mg/ml), and acepromazine maleate (10 mg/ml) in a 3:3:1 ratio, respectively. The mice were then euthanized by cervical dislocation Gastrocnemius muscle, liver, and most of one epididymal fat pad were excised and flash frozen. One whole fat pad was used immediately for fluorescence activated cell sorting (FACS) analysis and RNA isolation for qPCR. Part of one fat pad was immediately fixed in 10% neutral buffered formalin for histological studies.

Metabolic studies in mice – 16 week 60% HFD study

Insulin sensitivity in the mice was determined using a hyperinsulinemic euglycemic glucose clamp technique as previously described (12) with the following modifications: 1) cocktail of ketamine, xylazine, and acepromazine was used for anesthesia, as outline above 2) glucose tracer was infused at 2 μCi/hr, and 3) insulin was infused at 6 mU/kg/min. Plasma glucose specific activity, GDR, and HGO were

calculated as described above. The animals were allowed to recover. Seven days post-clamp procedure, mice were fasted for 8 hr and then anesthetized (cocktail). One lobe of the liver, one gastrocnemius muscle, and one and one-half pad of epididymal fat were tied off and collected. One whole pad of epididymal fat was used for FACS analysis as well as RNA isolation of subcellular fractions for qPCR. The remaining half pad of epididymal fat was divided in half (quarter of a pad). One quarter was flash-frozen, the other quarter was fixed in 10% neutral buffered formalin. The liver and muscle were flash-frozen. These samples represent the "basal treated" tissue samples. "Basal treated" blood was collected at the time of gastrocnemius muscle excision from blood that leaked from the femoral artery. Acute insulin stimulation was achieved by injection of 1.0 U/kg insulin into the inferior vena cava. After 5 minutes, tissues were harvested as above and blood was collected during the excision of the liver. No epididymal fat pad after insulin treatment was fixed in 10% neutral buffered formalin. These samples represent the "insulin treated" tissue samples.

Metabolic chamber analyses – 60% HFD study

Mice were started on HFD after 12 weeks of age. They were on diet for 12 weeks prior to being analyzed. Animals were allowed 48 hours to acclimatize to the metabolic chambers. Measurements were taken for three-12 hour dark cycles and two-12 hour light cycles. Analysis was provided by the University of California, San Diego School of Medicine Metabolic Resource Center.

Plasma and tissue analyses – 41% and 60% HFD study

Tissue lysates were analyzed by SDS-PAGE, western blotting and chemiluminescence and by ELISA (Meso Scale Discovery, Gaithersburg, MD). Signal intensities of chemiluminescence autoradiographs were densitometrically quantified using a digital Kodak 3D Imagestation and associated digital image analysis software (Kodak, New Haven, CT). IL-1β, IL-12p70, IFNγ, IL-6, IL-10, Cxcl1 and TNFα levels in plasma and tissue lysates were measured using a multiplex (7-plex) ELISA (Meso Scale Discovery). For SDS-PAGE and westernblotting analysis Phospho-Akt(Ser473) and Total Akt antibodies (Cell Signaling Technology, Beverly, MA) were used at 1:5000. Phospho-tyrosine antibody (BD Biosciences, San Jose, CA) was used at 1:10000.

Histological studies – two week 41% HFD study

Excised fat pads were immediately fixed in Zn-formalin overnight, transferred to 70% ethanol, and subsequently paraffin-embedded. Paraffin sections stained with hematoxylin and eosin were used for determining cell size, as previously described (Rieusset). All digital images of tissue sections were captured using the same microscope magnification. Microscopic fields with minimal non-adipocyte material were selected for quantitation of cell number per field. There was no apparent difference in non-adipocyte material in the sections between the mouse groups. Three fields were captured per mouse fat pad, from five mice in each group. Section images were visualized and cells per field image counted using ImageJ software (NIH freeware). Adipocyte size is represented by the inverse of the adipocyte number per field. Immunohistochemistry was performed

using a Mac-2 antibody (Cedarlane Laboratories, Ltd., Hornby, Ontario, Canada) to identify macrophages.

Staining analysis was performed at the Histology and Immunohistochemistry Resource at the Rebecca and John Moores UCSD Cancer Center.

Quantitative PCR

RNA from stromal vascular cells (SVCs) and adipocyte cells was extracted using Trizol (Invitrogen Corporation, Carlsbad, California). Reverse transcription was done using the iScript cDNA Synthesis Kit (Bio-Rad Laboratories, Hercules, California). Quantitative PCR (qPCR) was done using the iTaq SYBR Green Supermix With ROX (Bio-Rad Laboratories, Hercules, California). The OPN and IL-6 primers were used for both two and four week 60% HFD study as well as 16 week 60% HFD study and are as follows: mouseSPP1: forward, 5'–AGCCACAAGTTTCACAGCCACAAGG–3'; reverse, 5'–CTGAGAAATGAGCAGTTAGTATTCCTGC–3'; mouseIL-6: forward, 5'–CCAGAGATACAAAGAAATGATGG–3'; reverse, 5'–ACTCCAGAAGACCAGAGGAAAT–3'. Relative expression for the two and four week 60% study was determined by normalization to mouse GAPDH. mouseGAPDH: forward, 5'–AATGTGTCCGTCGTGGATCT–3'; reverse, 5'–CATCGAAGGTGGAAGAGTGG–3'. Relative expression for the 16 week study was determined by normalization to mouse RNA polymerase II. mouseRNA polymerase II: forward, 5'–GATCAACAATCAGCTGCGGCGG–3'; reverse, 5'–CCAGACTTCTGCATGGCACGGG–3'.

FACS analysis

The protocol to separate the SVF from the adipocyte fraction as well as to stain cells was followed as previously published (22). F4/80 conjugated with APC, CD11b with FITC, and CD11c with PE antibodies were used to stain the cells. All cells were analyzed the same day as tissue was excised. Staining analysis was performed at the Rebecca and John Moores UCSD Cancer Center, Flow Cytometry Resource.

Statistical analyses

Student's t-test and ANOVA with Tukey post-hoc test were used for statistical analyses. A p-value cutoff of 0.05 was used to determine significance after statistical tests.

RESULTS

Section 1. The effects of a two week 41% high fat diet on WT and OPN KO mice

1.1 OPN KO mice are protected from HFD-induced changes in insulin sensitivity

A hyperinsulinemic euglycemic clamp was performed on WT and OPN KO mice after two weeks of HFD or NC in order to determine the effects of the gene KO during the early onset of diet-induced insulin resistance. Marked changes in clamp values were observed for mice of both strains. For both HFD groups the GIR at clamp decreased when compared to their matched NCs. The OPN KO HFD mice had only a 19% decrease in GIR whereas the WT HFD group decreased by 73% (Figure 1A). Likewise, the WT HFD mice exhibited a 57% decrease in GDR at clamp versus the WT NC animals. The OPN KO mice on HFD had a 13% decrease in GDR when compared to their matched NC mice (Figure 1B). In addition, the HGO of the WT mice increased by 66% upon HFD-feeding while the HGO of the OPN KO HFD mice increased by 42% compared to their NC counterparts (Figure 1C).

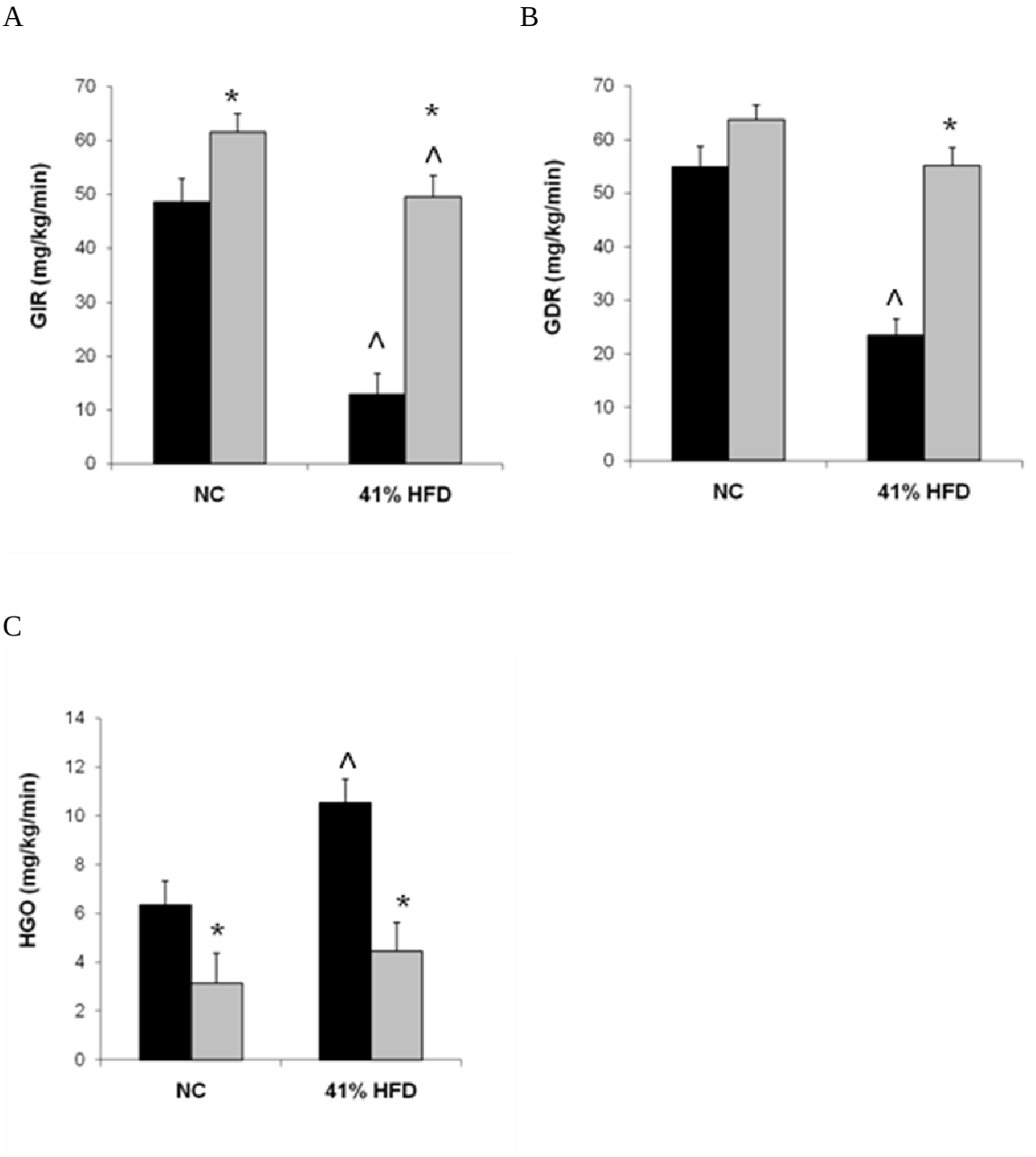

Figure 3. Liver and muscle insulin sensitivity after two weeks on 41% HFD. (A) GIR (B) GDR, (C) HGO as determined by hyperinsulinemic euglycemic clamp. WT mice (black bars) and OPN KO mice (gray bars) fed NC or 41% HFD for two weeks. N = 7-9 mice per group. Bars represent average values ± standard error of the mean. * $p<0.05$ vs. diet-matched WT, ^ $p<0.05$ vs. strain-matched NC.

1.2 Increased Akt phosphorylation in muscle and adipose tissue of KO mice

To examine the effects of OPN KO on insulin signal transduction (Figure 1) after HFD, Akt phosphorylation in muscle and two depots of WAT tissue was analyzed via acute insulin stimulation (Figure 4). The eWAT represents a visceral depot of adipose tissue, whereas the iWAT is a subcutaneous depot. OPN KO mice exhibited 58% greater insulin-stimulated Akt phosphorylation in muscle tissue compared to WT HFD mice. Similarly, the eWAT of OPN KO HFD mice had 73% more Akt phosphorylation than the matched WT mice after insulin stimulation. iWAT tissue did not show differences in Akt phosphorylation between strains.

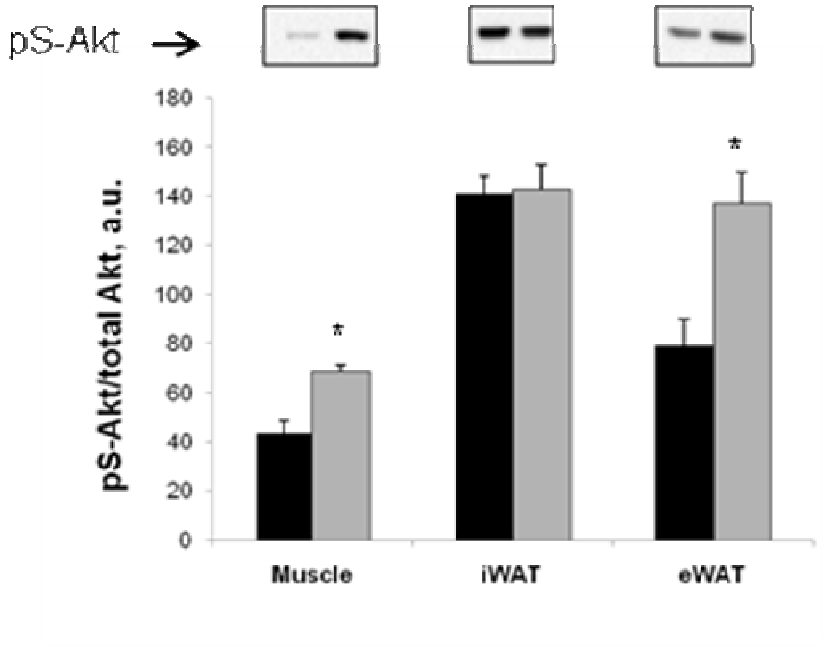

Figure 4. Akt phosphorylation in muscle and WAT tissues of 41% HFD mice after acute insulin stimulation. Acute insulin stimulation was done as described in the methods. Muscle is gastrocnemius, iWAT is inguinal WAT, eWAT is epididymal WAT. Values for graph were measured by ELISA. Representative western blots of each tissue are shown above the values. WT HFD mice (black bars), OPN KO HFD mice (gray bars). Bars represent average values $\pm$ standard error of the mean. N = 8-10 animals per group. * $p<0.05$ vs. matched-WT HFD group in respective tissue.

1.3 Decreased HFD-induced-hypertrophy in adipose tissue of OPN KO mice

The eWAT and iWAT were examined for cell size and macrophage content. It was found that adipose tissue hypertrophy due to HFD occurred in both strains, but this hypertrophy was mitigated in the OPN KO mice for both depots examined (Figure 5A-C). Overall fat pad weight did not differ between the strains (Figure 6), therefore decreases in cell numbers correlate with increased cell size. In the eWAT, adipocyte cell size more than doubled in the WT HFD mice, when compared to the NC mice (138% increase). In the same depot, OPN KO HFD mice had only a 67% increase in cell size. The blunted hypertrophy of the OPN KO HFD is even greater in the iWAT depot where the cell size increased by 29%. In contrast, an 81% increase was observed for the WT HFD animals.

The tissues were also examined for the presence of ATMs by use of a macrophage-specific marker Mac-2. Previous studies have shown that Mac-2 staining increases in obese mice (8). Both iWAT and eWAT were examined for number of crown-like structures as well as the overall number of Mac-2 stained cells. Neither type of fat pad showed differences between diets or strains in Mac-2 staining (data not shown).

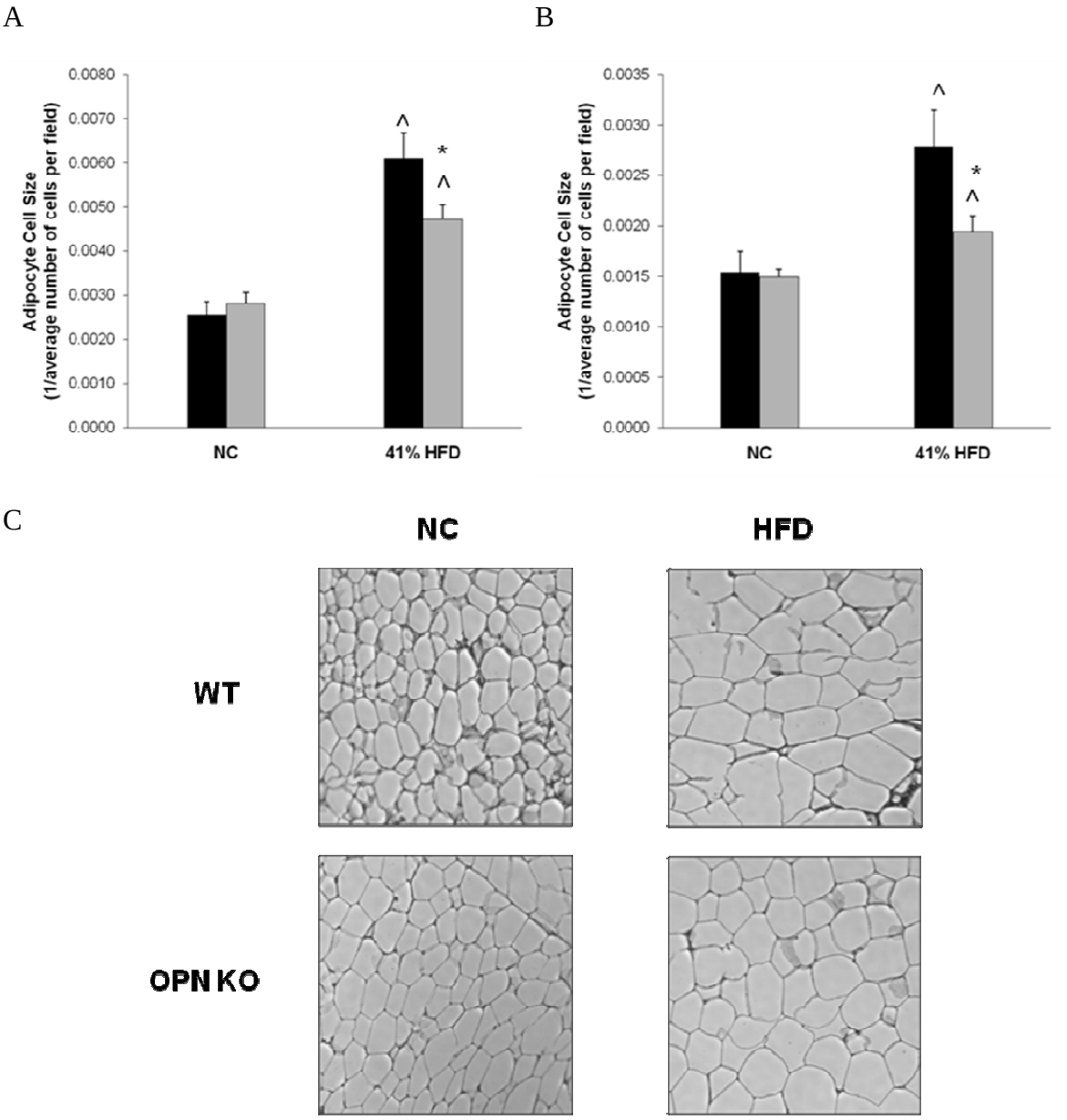

Figure 5. Adipocyte cell size in eWAT and iWAT. Cell size in (A) eWAT and (B) iWAT. 3 fields per animal were counted as described in methods. WT mice (black bars), OPN KO mice (gray bars). Bars represent average values ± standard error of the mean. N = 7 animals per group. * $p<0.05$ vs. diet-matched WT, ^ $p<0.05$ vs. strain-matched NC. (C) Representative fields from eWAT sections.

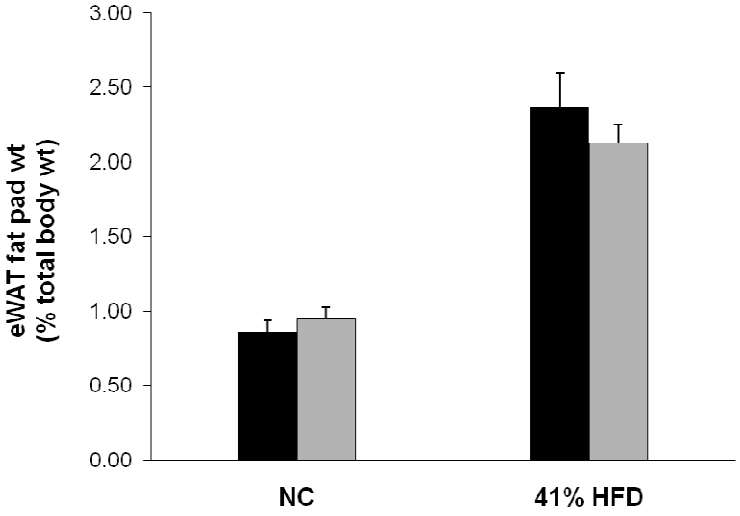

Figure 6. eWAT fat pad weight as a percentage of body weight after two weeks on 41% HFD. WT mice (black bars), OPN KO mice (gray bars). N = 8-9 animals per group. Bars represent average value ± standard error of the mean.

1.4 Increased pro-inflammatory cytokine levels in eWAT of WT HFD mice

Adipose tissue cytokine levels were measured in the eWAT tissue of the WT and OPN KO mice on both diets in order to further assess inflammation of the adipose tissue. Significant increases in IL-1β, IL-12p70, interferon γ (IFNγ), IL-6, and IL-10 were observed in eWAT lysates from HFD-fed WT mice (Figure 7). The levels of two other cytokines measured, Cxcl1 (KC) and TNFα, did not increase significantly after HFD, but showed a trend towards increased levels. Conversely, the eWAT lysates of OPN KO mice displayed a protection from increases in cytokine levels after HFD.

Figure 7. Expression of pro-inflammatory cytokine panel in eWAT after two weeks on HFD. Cytokine expression (ELISA) in both NC and 41% HFD WT mice (black bars) and OPN KO mice (gray bars). Bars represent average values $\pm$ standard error of the means. N = 8-10 animals per group. * $p<0.05$ vs. diet-matched WT, ^ $p<0.05$ vs. strain-matched NC.

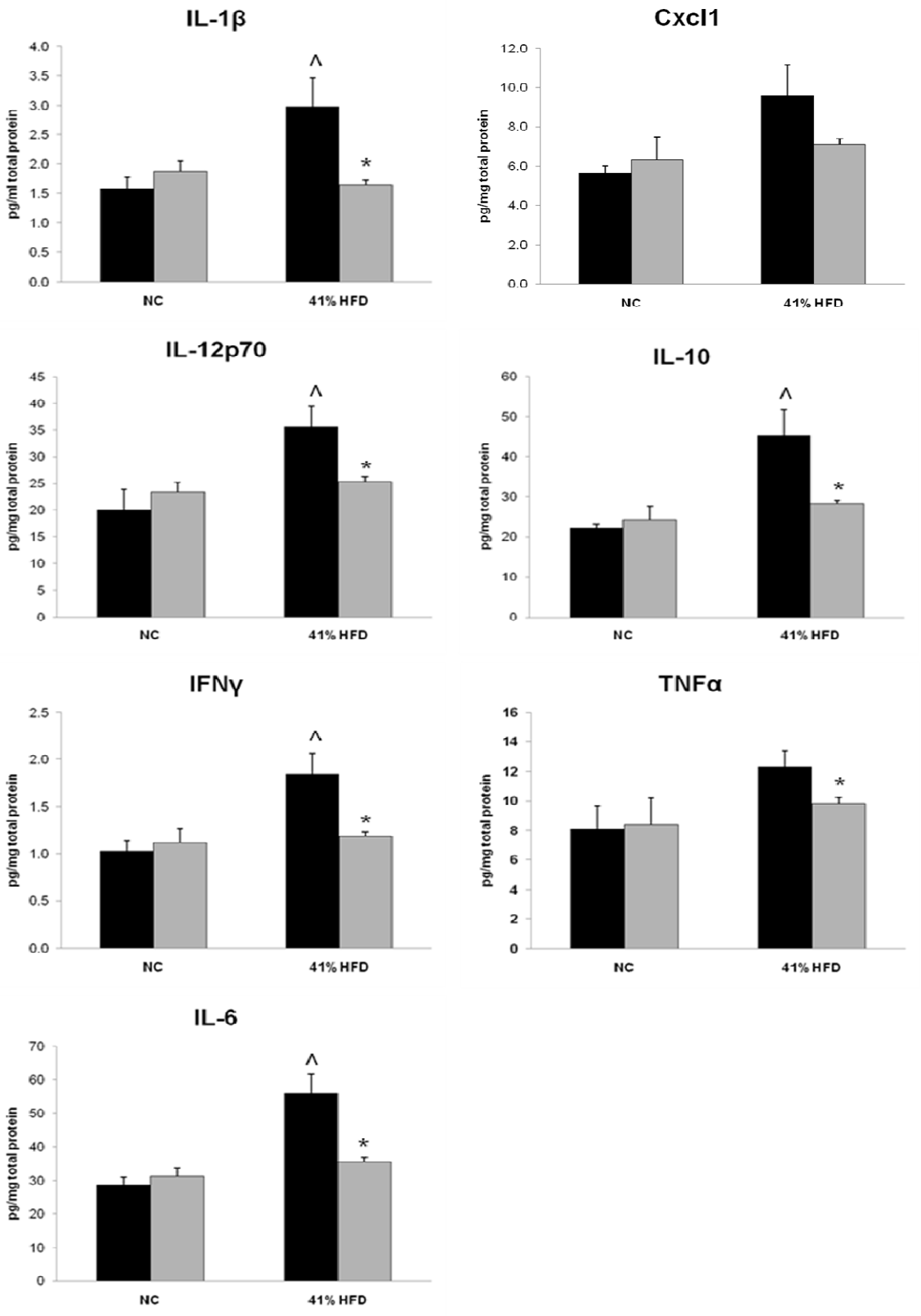
IL-1β
pg/ml total protein
4.0
3.5
3.0
2.5
2.0
1.5
1.0
0.5
0.0
^
*
NC
41% HFD
Cxcl1
pg/mg total protein
12.0
10.0
8.0
6.0
4.0
2.0
0.0
NC
41% HFD
IL-12p70
pg/mg total protein
45
40
35
30
25
20
15
10
5
0
^
*
NC
41% HFD
IL-10
pg/mg total protein
60
50
40
30
20
10
0
^
*
NC
41% HFD
IFNγ
pg/mg total protein
2.5
2.0
1.5
1.0
0.5
0.0
^
*
NC
41% HFD
TNFα
pg/mg total protein
16
14
12
10
8
6
4
2
0
*
NC
41% HFD
IL-6
pg/mg total protein
70
60
50
40
30
20
10
0
^
*
NC
41% HFD

1.5 No difference in plasma RBP4 levels between strains

Increased plasma levels of the adipokine RBP4 has been shown to correlate with insulin resistance in mice and humans (37). In order to determine whether the KO mice were protected from increased levels of RBP4 after HFD, plasma samples of the mice along with standard amounts of pure mouse RBP4 protein were run via western blot and RBP4 levels were measured densitometrically. No difference in RPB4 levels between the strains was found, but the OPN KO HFD mice displayed a trend towards decreased levels compared to the WT HFD mice (Figure 8).

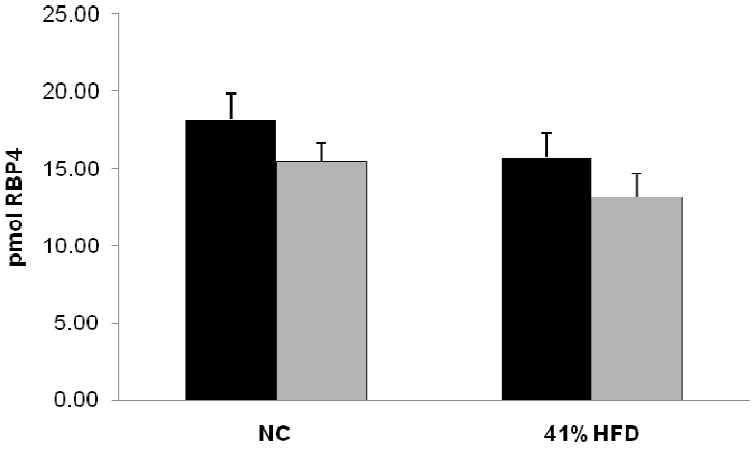

Figure 8. Plasma RBP4 levels after two weeks HFD. RBP4 levels in the plasma of both NC and 41% HFD WT (black bars) and OPN KO (gray bars) mice. Bars represent average values ± standard error of the mean. N = 6-14 animals per group.

1.6 Differential isomeric expression of OPN in eWAT

As a result of the increased levels of cytokines observed in the eWAT of the WT mice after HFD, a change in expression levels of OPN in the eWAT of the mice was expected. This was first assessed in eWAT lysates of WT NC and WT HFD mice that

had been on the 41% HFD for two weeks by ELISA. No difference in total OPN levels was detectable between the two groups (Figure 9). This was followed up by immunoblotting for OPN using a proprietary antibody, MOR6993 (Pfizer, La Jolla, CA), made against human and mouse OPN. This was done against WT NC mice as well as WT mice that had been on 41% HFD for two and four weeks (Figure 10). The results of this blot showed a diet-dependent mobility shift pattern of OPN. WT NC mice showed expression of OPN primarily in a band running at 40 kDa, whereas WT mice on either length of HFD displayed expression of an OPN isoform running at approximately 55 kDa. Consequently, when the expression of the 40 kDa and 55 kDa isomers were added together for total OPN expression for each diet type, no differences in total OPN expression were observed. This follows given the fact that the ELISA on OPN showed no changes in OPN levels among the WT NC and two week HFD (Figure 9).

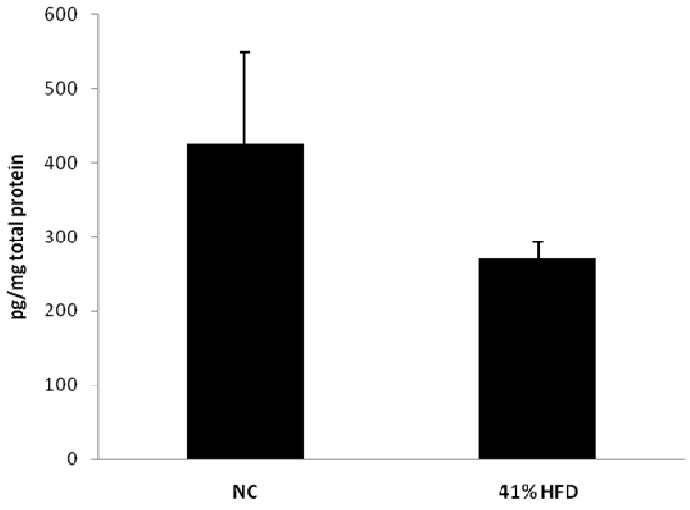

Figure 9. Expression of OPN protein in eWAT of WT mice. Level of OPN (pg) measured in both NC and 41% HFD mice. Bars represent average value ± standard error of the mean. N = 3-6 animals per group.

A

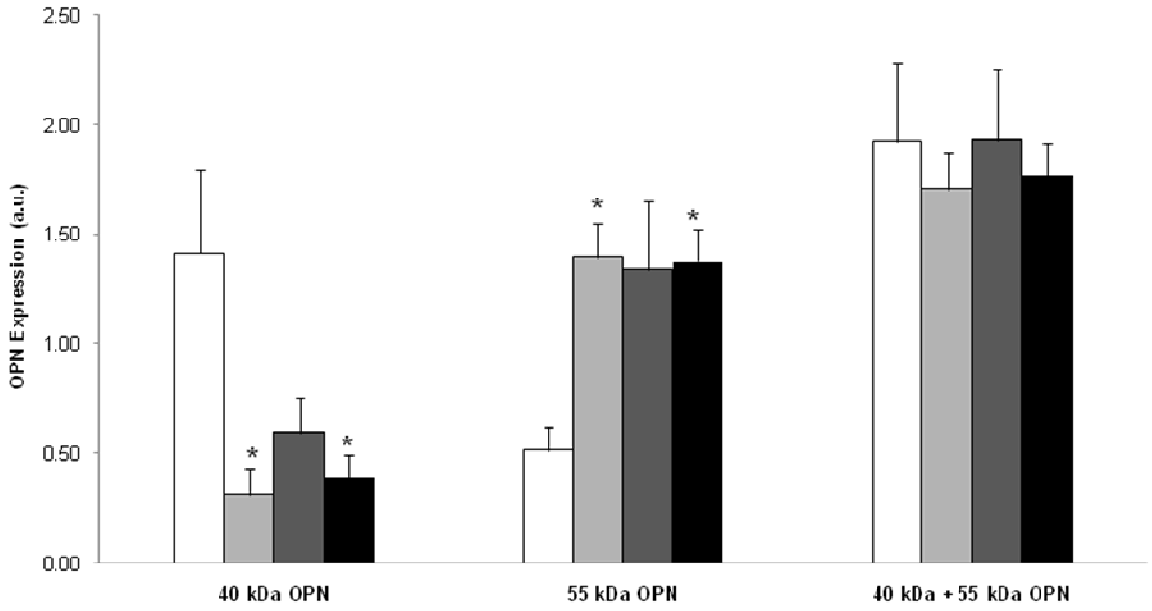

B

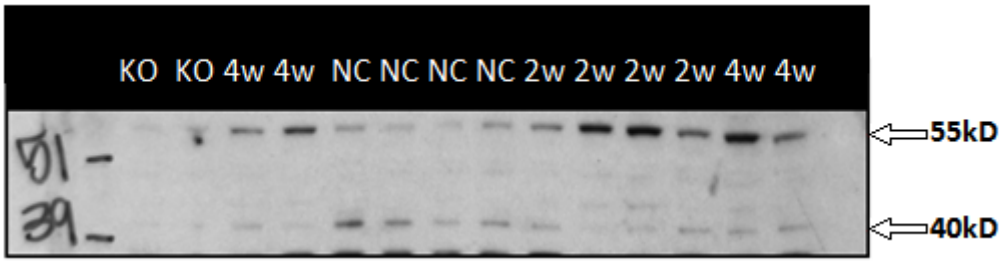

Figure 10. Differential OPN expression in eWAT. (A) Expression of 40 kDa, 55 kDa, and both 40 and 55 kDa (40+55) OPN isoforms in WT two week 41% HFD mice (light gray bars), four week 41% HFD mice (dark gray bars), two and four weeks 41% HFD mice (black bars), and NC mice (white bars). N = 4-8 animals per group. * $p<0.05$ vs. strain-matched NC mice. (B) Representative blot of 40 kDa and 55 kDa expression in WT eWAT tissue of NC, two week and four week HFD mice.

This section, in part is currently being prepared for submission for publication of the material. Divya Thapar, the thesis author, is a co-author of this material. I acknowledge Dorothy D. Sears, Justin G. Chapman, Jachelle M. Ofrecio, Philip D. Miles and Jaap G. Neels as co-authors of this material.

Section 2. The effects of a 60% high fat diet for 2-16 weeks on WT and OPN KO mice

2.1 OPN expression in SVF increases with two and four week HFD

In order to further determine changes in OPN expression in eWAT, qPCR was performed on the stromal vascular fraction (SVF) of the adipose tissue (Figure 11). It has previously been shown that macrophages and other immune cells express OPN (24). It follows that if there is increased infiltration by the triple-positive immune cells, there would be a subsequent increase in OPN expression. A 6-fold increased in OPN expression was observed in the WT mice after four weeks of HFD in the SVF. Although not significant, increased expression was observed after two weeks of HFD when compared to the NC mice. This localized expression pattern follows the data for the total OPN ELISA performed (Figure 9) as well as the differential isomeric expression data (Figure 10), both of which showed that after two and or four weeks of 41% HFD, no change in total OPN protein levels in eWAT as a whole is observed. OPN levels change only in particular subcellular fractions of the eWAT.

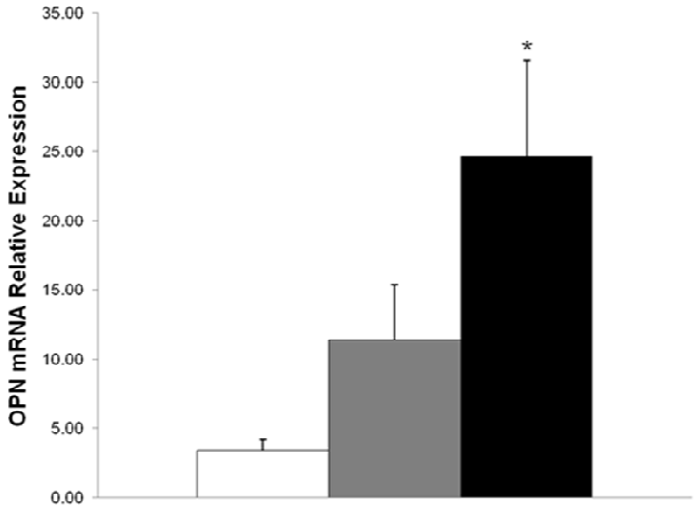

Figure 11. Relative OPN mRNA expression in SVF of eWAT. mRNA expression measured by qPCR in WT NC mice (white bar), two week HFD mice (gray bar), and four week HFD mice (black bar). Bars represent average of values ± standard error of the mean. N = 3 animals per group. * $p<0.05$ vs. strain-matched NC mice.

2.2 OPN KO mice have smaller percentage increase in triple-positive cells after HFD

FACS analysis was used to further determine immune cell infiltration into eWAT. The WT mice showed a marked increase in percentage of F4/80+, CD11b+ cells that are also CD11c+ after just two and four weeks on HFD when compared to their NC cohort (Figure 12). In contrast, the OPN KO mice exhibited a smaller percentage increase in triple-positive pro-inflammatory cells upon HFD.

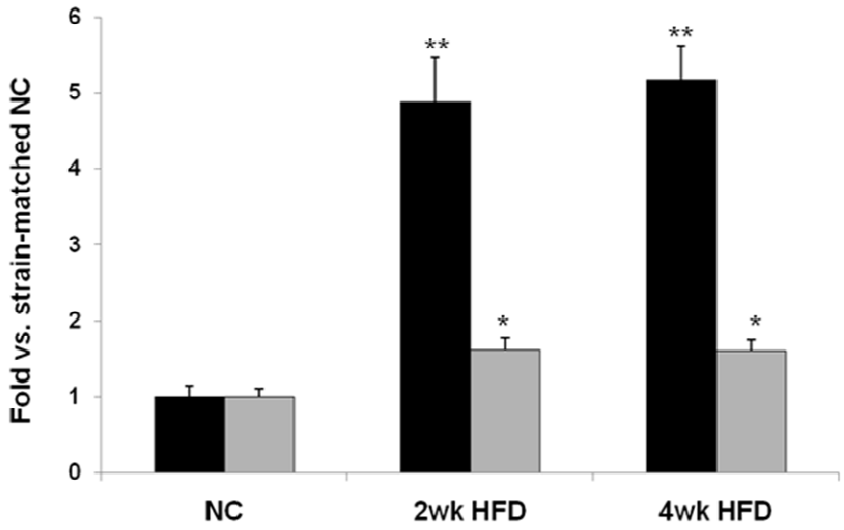

Figure 12. Percentage of F4/80+, CD11b+ cells that are also CD11c+. Staining of cells from WT (black bars) and OPN KO (gray bars) mice on NC, and two and four weeks HFD. Data normalized to strain-matched NC cohort. Bars represent average values ± standard error of the mean. N = 3-4 animals per group. * $p<0.05$ vs. strain-matched NC, ** $p<0.01$ vs. strain-matched NC.

2.3 No difference in food and water consumption, respiration, or activity between strains

Metabolic and physiological parameters were examined after 12 weeks on HFD. Oxygen consumption, carbon dioxide production, water and food consumption, and heat production were analyzed in addition to three different parameters of motor activity. The OPN KO mice on HFD had no differences in either metabolic criteria or motor activity when compared to their matched diet WT mice (Figure 13). No differences in any criteria were observed between either strain on NC (data not shown). It follows that the protection from insulin resistance and adipose tissue inflammation due to diet-induced obesity is not due to altered energy intake or expenditure by the KO strain.

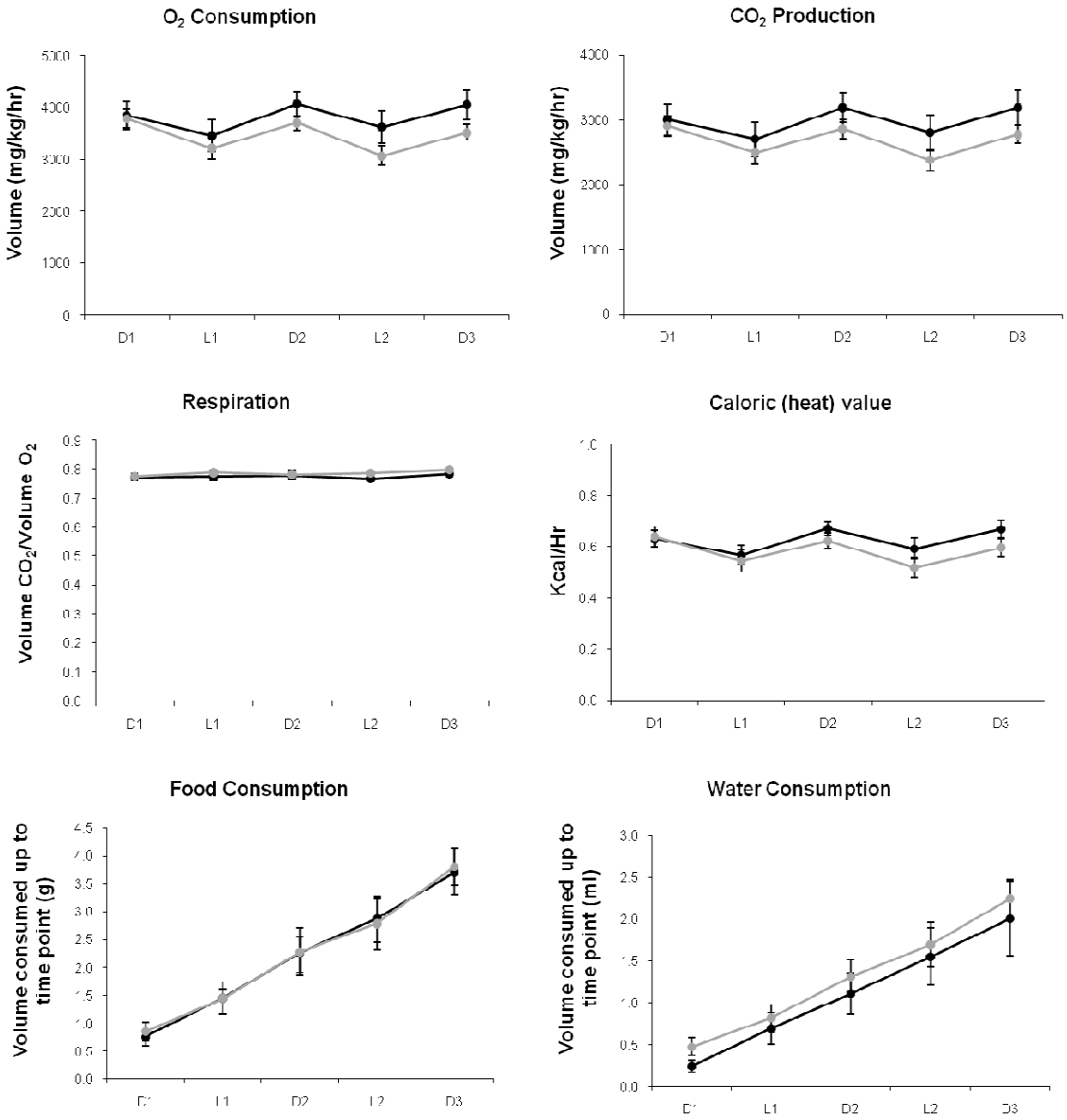

Figure 13. Metabolic and physical activity in OPN KO and WT mice. OPN KO HFD mice (gray lines) and WT HFD mice (black lines) were analyzed. Data points represent average values ± standard error of the mean. N = 6-7 animals per group. Student's t-test performed on each time point for statistical analysis.

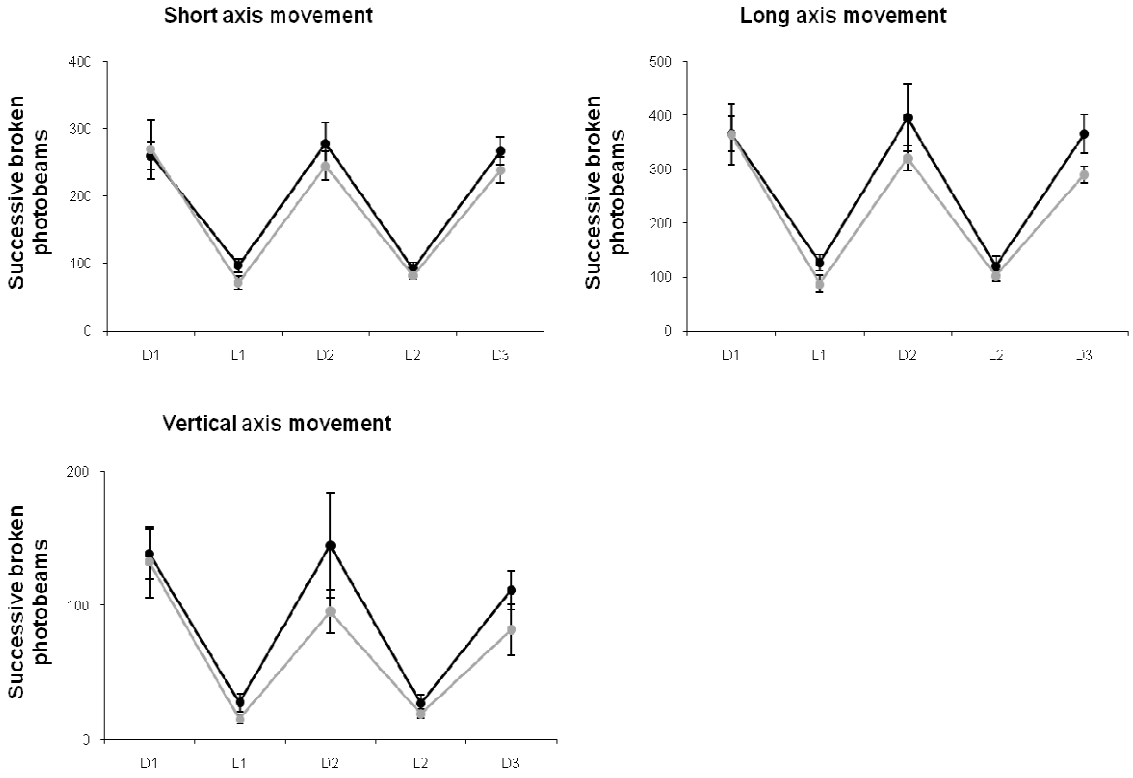

Figure 13 Continued. Metabolic and physical activity in OPN KO and WT mice.

2.4 Increased liver sensitivity to insulin remains after long-term HFD

Hyperinsulinemic euglycemic clamps were again utilized to determine the insulin sensitivity of the mice after 16 weeks on 60% HFD. The OPN KO HFD mice displayed decreased insulin resistance in the liver as compared to the WT HFD mice, as evidenced by lower HGO at clamp (Figure 14). There was no difference between the two strains in GDR or GIR, indicating no difference in muscle insulin sensitivity (data not shown).

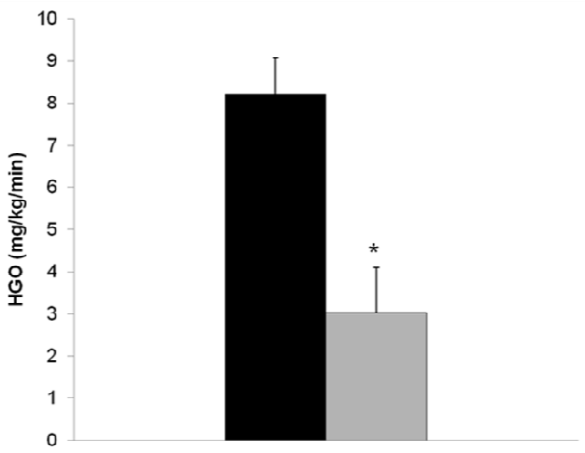

Figure 14. HGO after 16 week 60% HFD. WT HFD (black bars) and OPN KO HFD (gray bars) are shown. Bars represent average values ± standard error of the mean. N = 3 per group. * $p<0.05$ vs. diet-matched WT

2.5 Diminished Akt phosphorylation is inhibited in the muscle and of OPN KO mice after 16 weeks on HFD

Insulin signal transduction was again assessed in the mice after 16 weeks of HFD via acute insulin stimulation as outline above (Figure 15). Akt phosphorylation was significantly higher in the muscle tissue of the OPN KO mice on HFD in comparison to the WT mice. This indicates improved insulin signaling in muscle in OPN KO mice, despite no differences in muscle sensitivity observed by clamp.

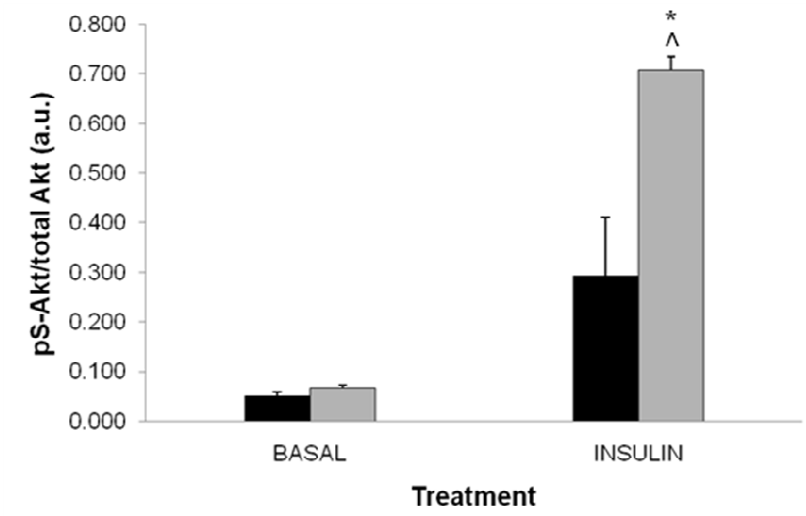

Figure 15. Insulin-stimulated Akt phosphorylation in muscle after 16 week HFD. Muscle tissue of WT HFD (black bars) and OPN KO HFD (gray bars) mice were examined after acute insulin stimulation as described. Bars represent average values ± standard error of the mean. N = 4-9 animals per group. * $p<0.05$ vs. insulin treatment-matched WT, ^ $p<0.05$ vs. strain-matched basal treatment.

2.6 OPN KO mice continue to be protected from diet-induced increases in IL-6 expression

IL- 6 expression in the eWAT of the WT and OPN KO HFD mice was examined as an indicator of inflammation of the adipose tissue of the mice. Expression was determined for the different fractions of the adipose tissue, SVF and adipocyte fraction. Although statistical significance was not achieved there was a distinct trend observed in both fractions of increased expression in the WT HFD animals that was blunted in the OPN KO animals (Figure 16).

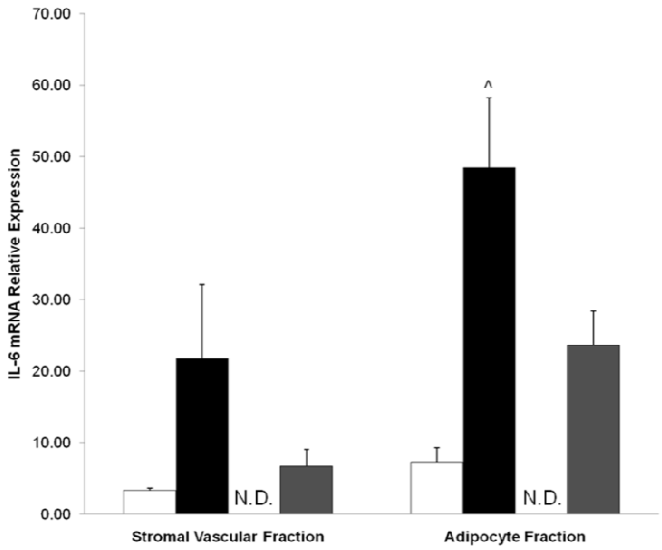

Figure 16. Relative expression of IL-6 in distinct eWAT fractions. WT NC mice (white bars), WT HFD mice (black bars), and OPN KO HFD mice (dark gray bars) expression was examined by qPCR. Expression in OPN KO NC mice was not determined (N.D.). Bars represent average values ± standard error of the mean. N = 2-9 animals per group. ^ $p<0.05$ vs. strain-matched NC.

2.7 No differences between strains in triple-positive pro-inflammatory cell infiltration after 16 week HFD

Infiltration into the eWAT of the triple-positive pro-inflammatory cells was again assessed by staining for F4/80, CD11b, and CD11c in FACS analysis. Unlike after 2 and 4 weeks HFD, no difference between the WT and OPN KO mice after 16 weeks on HFD was observed (data not shown).

2.8 OPN expression in adipose tissue remains elevated after 16 week HFD

OPN expression was again analyzed in the eWAT of the WT animals after long-term HFD. OPN expression was considerably higher in both the SVF and adipocyte fraction of the WT HFD mice (Figure 17). Statistical significance was not achieved for

the SVF, but a trend is quite evident, suggesting HFD does indeed induce OPN expression.

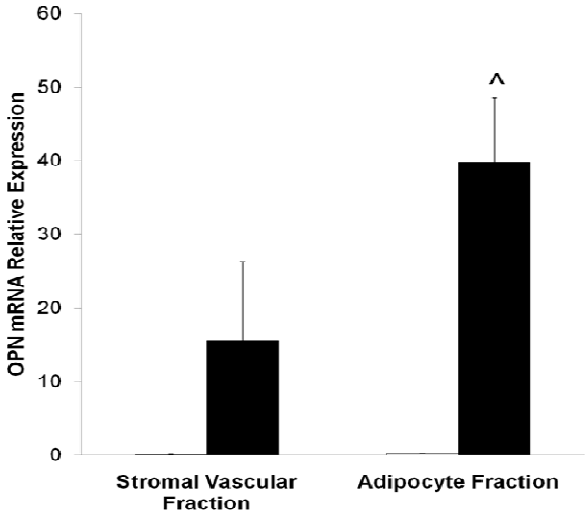

Figure 17. Relative expression of OPN in SV and adipocyte fractions after 16 week HFD. OPN expression in NC (white bars) and HFD (black bars) was determined by qPCR. Bars represent average values ± standard error of the mean. N = 2-9 animals per group. ^ $p<0.05$ vs. strain-matched NC.

This section, in part is currently being prepared for submission for publication of the material. Divya Thapar, the thesis author, is a co-author of this material. I acknowledge Dorothy D. Sears, Saswata Talukdar, and Jachelle M. Ofrecio as co-authors of this material.

DISCUSSION

The association of T2D and insulin resistance with inflammation is significant. OPN's function in immune cell activation led us to the current study of its possible role in contributing to insulin resistance. We first examined this in the early stages of insulin resistance from short-term diet-induced obesity using an OPN KO mouse model. We then investigated whether any protections offered after a short-term remained after long-term diet-induced obesity.

We found that the skeletal muscle and liver in WT mice on two week 41% HFD was more insulin resistant than compared to the OPN KO mice on 41% HFD. Increased skeletal muscle sensitivity was indicated by the KO mice having higher GDRs and GIRs during the hyperinsulinemic euglycemic clamp (Figure 3A-B). The higher GDR indicates that with the same dose of insulin, the muscle of the OPN KO mice is taking up more glucose than the muscle of the WT mice. Consequently, the GIR of the KO mice is also higher. More glucose being taken up by the muscle requires more glucose to be infused exogenously to remain at euglycemia. This further implicates greater insulin sensitivity of the muscle of OPN KO mice. Impaired insulin sensitivity in the liver of the WT HFD mice was determined by them having a higher HGO at clamp in comparison to the OPN KO HFD mice (Figure 3C). Decreased HGO means their livers are more sensitive to the hyperinsulinemic state and responding appropriately by desisting glucose production. After 16 weeks of 60% HFD, increased hepatic insulin sensitivity remained in the OPN KO mice (Figure 14). Protection from insulin resistance in the muscle was not observed via glucose clamp (data not shown).

Another indicator of insulin resistance that we looked at was Akt phosphorylation after acute insulin-stimulation. After two weeks on HFD, diminished insulin signaling was observed in muscle and eWAT of WT HFD animals and was blunted in OPN KO HFD mice (Figure 4). The OPN KO mice after 16 weeks HFD, showed increased Akt phosphorylation in their muscle compared to the WT mice (Figure 15). This indicates an increased muscle sensitivity phenotype in the OPN KO mice, despite no differences being detected by clamp. Therefore, the defense of the OPN KO against inhibition of insulin signaling in the muscle brought about by HFD is maintained despite length of diet. There was no difference between the strains in Akt phosphorylation in eWAT after the 16 week diet (data not shown).

Adipose tissue hypertrophy was measured as one indicator of adipose tissue inflammation. Cell size in both the eWAT and iWAT was recorded. We found that even after just two weeks on HFD, the adipose tissue of WT HFD mice had undergone significant hypertrophy in both depots of WAT (Figure 5A-C). In the eWAT, cell size more than doubled after HFD. Measurements of the OPN KO mice showed definite diet-induced adipose tissue hypertrophy. However, in comparison to the extent of hypertrophy in the WT mice after HFD, hypertrophy in the adipose tissue was blunted in the OPN KO mice. This may be, in part, why KO mice are more protected from inflammation of the adipose tissue. Decreased hypertrophy indicates less of a hypoxic environment for the adipocytes as well as less lipolysis and FFA secretion, which have previously been shown to activate inflammatory pathways (21, 30, 39). OPN expression decreases in a time-dependent manner during the adipocyte differentiation process (36). Preliminary data also suggest that OPN expression increases towards the end of the

differentiation process in 3T3-L1 preadipocytes (data not shown). Given that OPN -/- preadipocytes lack OPN expression, it is possible that the preadipocytes from OPN KO mice are unable to differentiate into adipocytes that can carry as much of a lipid load as WT adipocytes. This could protect OPN KO adipocytes from the extent of hypertrophy observed in WT adipocytes.

In order to further establish the extent of inflammation of the eWAT, the second indicator of inflammation that we examined was cytokine expression. After only two weeks of HFD, the WT mice showed a significant increase in expression of IL-6, IL-1β, IL-10, IFNγ, and IL-12p70. OPN KO mice exhibited a diminished response to diet-induced expression increases (Figure 7). This further proves that the adipose tissue of OPN KO HFD animals at two weeks has decreased inflammation. In order to verify that this protection remained after the 16 week length of diet, expression of IL-6 was used as an indication of overall pro-inflammatory cytokine expression. We found that the OPN KO HFD mice had a strong trend towards decreased IL-6 expression in the SVF and reached significance in the adipocyte fraction (Figure 16). Therefore, diminished inflammation of the adipose tissue is protected in KO mice after the longer diet.

We also examined RBP4 expression in the plasma an indicator of inflammation, but no differences were observable between strains or diets (Figure 8). This indicates that although the WT mice are insulin resistant after only two weeks of HFD, the resistance has not progressed enough, in this course of diet, to cause alterations in RBP4 expression.

OPN expression within the WT mice was then examined because we expected that the adipose tissue of the NC mice should express less OPN given that OPN has

inflammatory-cytokine-like properties, and the NC mice should not be in an inflammatory state. When OPN was measured in eWAT as a whole, no difference in expression was observed between diets (Figure 9). But when expression was measured by SDS-PAGE, we saw a significant mobility-shift in OPN expression that is dependent on diet. We found that there were two different isoforms of OPN, what we are calling the 40 and 55 kDa, and that WT NC mice predominantly express the 40 kDa isoform. There is a shift in expression to the 55 kDa isoform even after just two weeks on HFD (Figure 10). The total expression of OPN did not appear to change given that the sum of the 40 kDa and 55 kDa expression was not different between diets. This affirms why differences in OPN in total eWAT tissue by ELISA were not observable. The vast extent of PTM that OPN is able to undergo, there are multiple mechanism by which OPN could be altered. MMP and thrombin cleavage sites in the OPN amino acid sequence lie within integrin-binding motifs (29), so cleavage at these sites could produce isoforms of OPN have changes in signaling capabilities. Being able to/not being able to signal through a specific integrin could be required for propagation of the OPN inflammatory signal. WT NC mice could express an isoform of OPN that is unable to signal in an inflammatory manner or is diminished in its inflammatory signaling capabilities in the adipose tissue. OPN could also be the target of upstream kinases that are also sensitive to insulin signaling. This would cause a specific phosphorylation pattern of OPN that could activate it in a more pro-inflammatory manner. Any change in signaling ability due to this PTM is important to determine the exact role of OPN in attenuating insulin resistance and inflammation.

We further examined whether there were diet-induced changes in expression of OPN on a subcellular level. After two and four weeks on 60% HFD, we observed marked increase of OPN in the SVF of the eWAT (Figure 11). This increase in OPN expression remained after 16 weeks of 60% HFD, and was also found to be true in the adipocyte fraction (Figure 17). The increased cytokine expression in the eWAT of the WT HFD mice indicates macrophage or pro-inflammatory immune cell infiltration. Because OPN is known to act as a macrophage chemotactic agent, it could be that macrophages and adipocytes within the adipose tissue are over expressing OPN in order to cause more macrophage migration into the adipose tissue as a response to increased adipocyte cell death occurring.

Macrophage infiltration of the adipose tissue after two weeks on 41% HFD was assessed to determine the role of OPN in macrophage invasion of the adipose tissue during inflammation and insulin resistance. By histological staining, no difference in macrophage number or content was determined between the strains (data not shown). When stained by FACS in a two and four week 60% HFD model, it was found that the percentage of F4/80+, CD11b+, CD11c- cells that were also CD11c+ after HFD increases and this increase is diminished in the OPN KO mice (Figure 12). By enhancing triple-positive pro-inflammatory cell infiltration, OPN could function to further increase the inflammation of the adipose tissue and abet in the development and progression of insulin resistance. No differences in triple-positive pro-inflammatory cells were observed between the strains after 16 weeks HFD. Therefore it could be that OPN only protects from immune cell invasion during the early stages of insulin resistance. Given that inflammatory cytokine expression remains inhibited in the OPN KO mice after 16 week

HFD (Figure 16), OPN could function to alter the inflammatory state of the triple-positive cells rather than affect cell migration.

Finally, we examined whether the protections from insulin resistance and inflammation in the OPN KO HFD mice were due to increase physical activity or other metabolic parameters that cause increased energy expenditure or intake. This was done in WT and OPN KO mice after 12 weeks of 60% HFD. No differences in respiration, caloric heat value, food and water intake, and motor activity were observed between the strains (Figure 13). This indicates that OPN KO does not exert its protections through increased metabolism or movement.

In summary, the OPN KO provides protection in multiple insulin-target tissues, including muscle and liver, from insulin resistance. This protection remains even after long-term diet-induced obesity. OPN KO mice also have decreased adipose tissue inflammation as measured by hypertrophy, cytokine expression, and OPN expression. Decreased infiltration of the adipose tissue by triple-positive pro-inflammatory cells as well as differences in inflammatory state of the triple-positive pro-inflammatory cells in the KO animals provides a possible reason for the differences in cytokine expression. Differential expression of OPN isomers dependent on diet could provide a mechanism by which this occurs. OPN potentially serves as a novel therapeutic target for the treatment of insulin resistance and T2D.

REFERENCES

1. Agnholt J, Kelsen J, Schack L, Hvas CL, Dahlerup JF, and Sorensen ES. Osteopontin, a protein with cytokine-like properties, is associated with inflammation in Crohn's Disease. *Scand J Immunol* 65(5): 453-60, 2007.

2. Agnihotri R, Crawford HC, Haro H, Matrisian LM, Havrda MC, and Liaw L. Osteopontin, a novel substrate for matrix metalloproteinase-3 (stromelysin-1) and matrix metalloproteinase-7 (matrilysin). *J Biol Chem* 276(30): 28261-7, 2001.

3. Alessi DR, James SR, Downes CP, Holmes AB, Gaffney PR, Reese CB, and Cohen P. Characterization of a 3-phosphoinositide-dependent protein kinase which phosphorylates and activates protein kinase Balpha. *Curr Biol* 7(4): 261-9, 1997.

4. Asano T, Fujishiro M, Kushiyama A, Nakatsu Y, Yoneda M, Kamata H, and Sakoda H. Role of phosphatidylinositol 3-kinase activation on insulin action and its alteration in diabetic conditions. *Biol Pharm Bull* 30(9): 1610-6, 2007.

5. Berkowitz K, Peters R, Kjos SL, Goico J, Marroquin A, Dunn ME, Xiang A, Azen S, and Buchanan TA. Effect of troglitazone on insulin sensitivity and pancreatic beta-cell function in women at high risk for NIDDM. *Diabetes* 45(11): 1572-9, 1996.

6. Bruemmer D, Collins AR, Noh G, Wang W, Territo M, Arias-Magallona S, Fishbein MC, Blaschke F, Kintscher U, Graf K, Law RE, and Hsueh WA. Angiotensin II-accelerated atherosclerosis and aneurysm formation is attenuated in osteopontin-deficient mice. *J Clin Invest* 112(9): 1318-31, 2003.

7. Centers for Disease Control and Prevention. National diabetes fact sheet: general information and national estimates on diabetes in the United States, 2007. Atlanta, GA: *U.S. Department of Health and Human Services*, 2008.

8. Cinti S, Mitchell G, Barbatelli G, Murano I, Ceresi E, Faloia E, Wang S, Fortier M, Greenberg AS, and Obin MS. Adipocyte death defines macrophage localization and function in adipose tissue of obese mice and humans. *J Lipid Res* 46: 2347-2355, 2005.

9. Denhardt DT, Giachelli CM, and Rittling SR. Role of osteopontin in cellular signaling and toxicant injury. *Annu Rev Pharmacol Toxicol* 41: 723-49, 2001.

10. Ehrmann DA, Schneider DJ, Sobel BE, Cavaghan MK, Imperial J, Rosenfield RL, and Polonsky KS. Troglitazone improves defects in insulin action, insulin secretion, ovarian steroidogenesis, and fibrinolysis in women with polycystic ovary syndrome. *J Clin Endocrinol Metab* 82(7): 2108-16, 1997.

11. Gunton JE, Kulkarni RN, Yim S, Okada T, Hawthorne WJ, Tseng YH, Roberson RS, Ricordi C, O'Connell PJ, Gonzalez FJ, and Kahn CR. Loss of ARNT/HIF1beta mediates altered gene expression and pancreatic-islet dysfunction in human type 2 diabetes. *Cell* 122(3): 337-49, 2005.

12. Hevener AL, Reichart D, Janez A, and Olefsky J. Thiazolidinedione treatment prevents free fatty acid-induced insulin resistance in male wistar rats. *Diabetes* 50(10): 2316-22, 2001.

13. Hotamisligil GS. Inflammation and metabolic disorders. *Nature* 444(7121): 860-7, 2006

14. Hotamisligil GS, Shargill NS, and Spiegelman BM. Adipose expression of tumor necrosis factor-alpha: direct role in obesity-linked insulin resistance. *Science* 259(5091): 87-91, 1993.

15. Hou P, Troen T, Ovejero MC, Kirkegaard T, Andersen TL, Byrjalsen I, Ferreras M, Sato T, Shapiro SD, Foged NT, and Delaisse JM. Matrix metalloproteinase-12 (MMP-12) in osteoclasts: new lesson on the involvement of MMPs in bone resorption. *Bone* 34(1): 37-47, 2004.

16. Hu DD, Hoyer JR, and Smith JW. Characterization of the interaction between integrins and recombinant human osteopontin. *Ann N Y Acad Sci* 760: 312-4, 1995.

17. Jager J, Gremeaux T, Cormont M, Marchand-Brustel Y, and Tanti JF. Interleukin-1beta-induced insulin resistance in adipocytes through down-regulation of insulin receptor substrate-1 expression. *Endocrinology* 148(1): 241-51, 2007.

18. Kido Y, Burks DJ, Withers D, Bruning JC, Kahn CR, White MF, and Accili D. Tissue-specific insulin resistance in mice with mutations in the insulin receptor, IRS-1, and IRS-2. *J Clin Invest* 105(2): 199-205, 2000.

19. Kopp HP, Kopp CW, Festa A, Krzyzanowska K, Kriwanek S, Minar E, Roka R, and Schernthaner G. Impact of weight loss on inflammatory proteins and their association with the insulin resistance syndrome in morbidly obese patients. *Arterioscler Thromb Vasc Biol* 23(6): 1042-7, 2003.

20. Lai L, Alaverdi N, Maltais L, and Morse-III HC. Mouse cell surface antigens: nomenclature and immunophenotyping. *J Immunol* 160(8): 3861-8, 1998.

21. Nguyen MT, Satoh H, Favelyukis S, Babendure JL, Imamura T, Sbodio JI, Zalevsky J, Dahiyat BI, Chi NW, and Olefsky JM. JNK and tumor necrosis factor-alpha mediate free fatty acid-induced insulin resistance in 3T3-L1 adipocytes. *J Biol Chem* 280(42): 35361-71, 2005.

22. Nguyen MT, Favelyukis S, Nguyen AK, Reichart D, Scott PA, Jenn A, Lui-Bryan R, Glass CK, Neels JG, and Olefsky JM. A subpopulation of macrophages infiltrates hypertrophic adipose tissue and is activated by free fatty acids via Toll-like receptors 2 and 4 and JNK-dependent pathways. *J Biol Chem* 282(48): 35279-92, 2007.

23. Nolan JJ, Ludvik B, Beerdsen P, Joyce M, and Olefsky J. Improvement in glucose tolerance and insulin resistance in obese subjects treated with troglitazone. *N Engl J Med* 331(18): 1188-93, 1994.

24. Nomiyama T, Perez-Tilve D, Ogawa D, Gizard F, Zhao Y, Heywood EB, Jones KL, Kawamori R, Cassis LA, Tschop MH, and Breummer D. Osteopontin mediates obesity-induced adipose tissue macrophage infiltration and insulin resistance in mice. *J Clin Invest* 117(10): 2877-88, 2007.

25. Olefsky JM. Treatment of insulin resistance with peroxisome proliferator-activated receptor gamma agonists. *J Clin Invest* 106(4): 467-72, 2000.

26. Reaven GM. Role of insulin resistance in human disease (syndrome X): an expanded definition. *Annu Rev Med* 44: 121-31, 1993.

27. Rieusset J, Touri F, Michalik L, Escher P, Desvergne B, Niesor E, and Wahli W. A new selective peroxisome proliferator-activated receptor gamma antagonist with antiobesity and antidiabetic activity. *Mol Endocrinol* 16(11): 2628-44, 2002.

28. Rodriguez, A., Catalan, V., Gomez-Ambrosi, J., and Fruhbeck, G. Visceral and subcutaneous adiposity: are both potential therapeutic targets for tackling the metabolic syndrome? *Curr. Pharm. Des.***13**:2169–2175, 2007.

29. Scatena M, Liaw L, and Giachelli CM. Osteopontin: a multifunctional molecule regulating chronic inflammation and vascular disease. *Arterioscler Thromb Vasc Biol* 27(11): 2302-9, 2007.

30. Schenk S, Saberi M, and Olefsky JM. Insulin sensitivity: modulation by nutrients and inflammation. *J Clin Invest* 118(9): 2992-3002, 2008.

31. Spiegelman BM. PPAR-gamma: adipogenic regulator and thiazolidinedione receptor. *Diabetes* 47(4): 507-14, 1998.

32. Tilg H, and Moschen AR. Inflammatory mechanisms in the regulation of insulin resistance. *Mol Med* 14(3-4): 222-31, 2008.

33. Weber GF, Ashkar S, Glimcher MJ, Cantor H. Receptor-ligand interaction between CD44 and osteopontin (Eta-1). *Science* 271(5248): 509-12, 1996.

34. Weisberg SP, Hunter D, Huber R, Lemieux J, Slaymaker S, Vaddi K, Charo I, Leibel RL, and Ferrante AW Jr. CCR2 modulates inflammatory and metabolic effects of high-fat feeding. *J Clin Invest* 116(1): 115-24, 2006.

35. Wild S, Roglic G, Green A, Sicree R, and King H. Global prevalence of diabetes: estimates for the year 2000 and projection for 2030. *Diabetes Care* 27: 1047-53, 2004.

36. Yang DC, Tsay HJ, Lin SY, Chiou SH, Li MJ, Chang TJ, and Hung SC. cAMP/PKA regulates osteogenesis, adipogenesis and ratio of RANKL/OPG mRNA expression in mesenchymal stem cells by suppressing leptin. *PLoS ONE* 3(2):e1540, 2008.

37. Yang Q, Graham TE, Mody N, Preitner F, Peroni OD, Zabolotny JM, Kotani K, Quadro L, and Kahn BB. Serum retinol binding protein 4 contributes to insulin resistance in obesity and type 2 diabetes. *Nature* 436(7049): 356-62, 2005.

38. Yu XQ, Nikolic-Paterson DJ, Mu W, Giachelli CM, Atkins RC, Johnson RJ, and Lan HY. A functional role for osteopontin in experimental crescentic glomerulonephritis in the rat. *Proc Assoc Am Physicians* 110(1): 50-64, 1998.

39. Yuan M, Konstantopoulos N, Lee J, Hansen L, Li ZW, Karin M, and Shoelson SE. Reversal of obesity- and diabetes-induced insulin resistance with salicylates or targeted disruption of Ikkbeta. *Science* 293(5535): 1673-7, 2001.